Self-assembled broadband plasmonic nanoparticle arrays for sensing applications

R. Verre,[a] K. Fleischer, O. Ualibek, and I. V. Shvets
Centre for Research on Adaptive Nanostructures and Nanodevices (CRANN), School of Physics, Trinity College of Dublin, Dublin 2, Ireland

(Received 19 August 2011; accepted 2 December 2011; published online 17 January 2012)

Highly ordered noble metal nanoparticle (NP) arrays are produced using a glancing angle deposition on stepped substrates. The versatility of the technique is demonstrated by depositing different metals, resulting in shifts of the resonance positions. The behaviour of the NP arrays grown is predicted by a dipolar model, and it is measured using reflectance anisotropy spectroscopy (RAS). Fine tuning of the resonances can be finally realised by selecting the deposition parameters. The combined application of both RAS and deposition at glancing angles provides a unique tool to grow NP arrays with the tunable plasmonic resonances in the entire visible range. © *2012 American Institute of Physics*. [doi:10.1063/1.3674982]

Metallic nanoparticle (NP) arrays have proven to be of fundamental importance for optoelectronic applications[1] and improved solar cells.[2] Such interacting metallic systems have been intensely investigated as templates for surface enhanced spectroscopy.[3,4] For these spectroscopic techniques, the resonant energy of the structures needs to match the energy of the exciting laser.[5] If the interparticle separation is smaller than the average NP diameter,[6] the electric field in the interstitial space is enhanced at resonance by orders of magnitude.[7]

The required NP arrangements can be readily obtained using lithographic techniques,[1] but these are unsuitable for the production of large scale active areas. Typical colloidal processes could be a solution,[8] but ordered deposition onto a substrate is required. The resulting optical spectra depend also on the parameters governing the coupling between NPs and on the morphology of the resulting structures. These growth methods are material specific and thus require unique preparation recipes, depending on the material utilised. Glancing angle deposition of adatoms can provide a possible solution (see Fig. 1).[9–14] A collimated adatom flux is directed towards the steps, which act as preferential growth sites. Adatoms then diffuse along the steps and coalesce, forming NP arrays. This self-assembled technique is simple, easily scalable, and mainly dependent on geometrical considerations. It is then conceptually independent of the deposition material. This letter demonstrates that NP arrays of different materials can be produced using this deposition method. The resulting resonances can be tuned over the whole visible range once the material choice is combined with different deposition parameters. At the same time, reflectance anisotropy spectroscopy (RAS) can be used to monitor, *in situ*, the evolution of resonance profiles during the growth. Structures with a particular resonance energy suitable for enhancements spectroscopy can then be obtained following this route.

Advantages in a material independent production method of NP arrays can be readily demonstrated by simulations. The anisotropic optical response can be reproduced by modelling each identical NP as a supported ellipsoid placed on a rectangular lattice. Once the dimensions involved are much smaller than the wavelength of light, the NP layer can be approximated as a continuous layer having an effective anisotropic in-plane dielectric function,[12]

$$\varepsilon_{L,i} = \varepsilon_m \left(1 + \frac{\varepsilon_m - \varepsilon_s}{\varepsilon_s + L_i^*(\varepsilon_m - \varepsilon_s)}\right), \tag{1}$$

where $i = (x,y)$, ε_s, and ε_m are the dielectric functions of the surrounding medium and of the metal, respectively. The standard shape depolarization factor L_i (Ref. 15) is modified in Eq. (1) to $L_i^* = L_i + \beta V$, thus taking into account the NP interaction and substrate effects through the β_i coefficients and the NP volume V (Refs. 11 and 14). If ω_P and Γ are the free electron plasma frequency and the scattering rate of the metallic NP, respectively, the dielectric function can be modelled as $\varepsilon = \varepsilon_\infty + \omega_p^2/(\omega^2 + i\omega\Gamma) + \varepsilon_{IB}$, where the core electrons contribution ε_∞ and interband transitions ε_{IB} are explicitly included. The resonance frequency can be found at the poles of Eq. (1), where

$$\omega_{res,i} = \sqrt{\frac{\omega_p^2}{(\varepsilon_\infty + \varepsilon_{IB}) + \left(\frac{L_i^*}{1-L_i^*}\right)\varepsilon_s} - \Gamma^2}. \tag{2}$$

The resonance frequency of Eq. (2) depends on three factors: the dielectric function of the surrounding medium ε_s, the

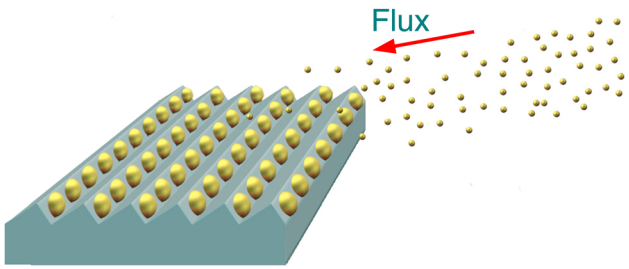

FIG. 1. (Color online) A schematic view of the deposition technique: a flux of collimated adatoms is sent towards the surface at a glancing angle of incidence and coalesces on the step of a patterned surface, forming NP arrays.

[a]Electronic mail: rverre@tcd.ie.

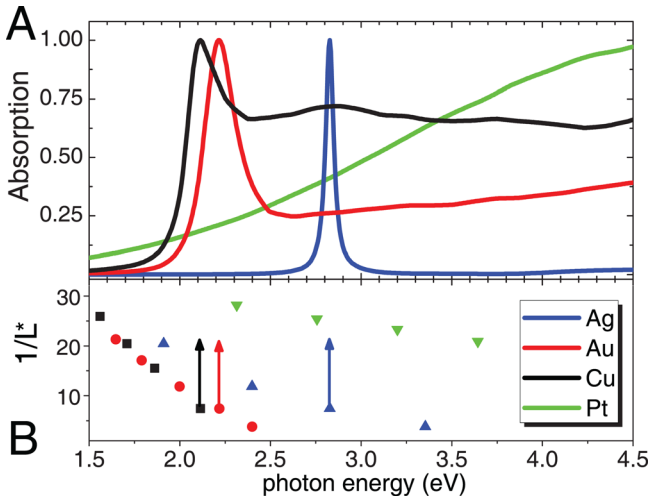

FIG. 2. (Color online) (a) Normalized absorption profiles of metal NP arrays. During the simulations, the light was sent along the array axis and the tabulated bulk dielectric functions were utilised.[16,17] (b) The plasmonic energy position, for different metals, as a function of $1/L^*$. The arrows indicate the positions of the peaks in (a). Shifts in the resonance can be obtained using different metals and different geometries.

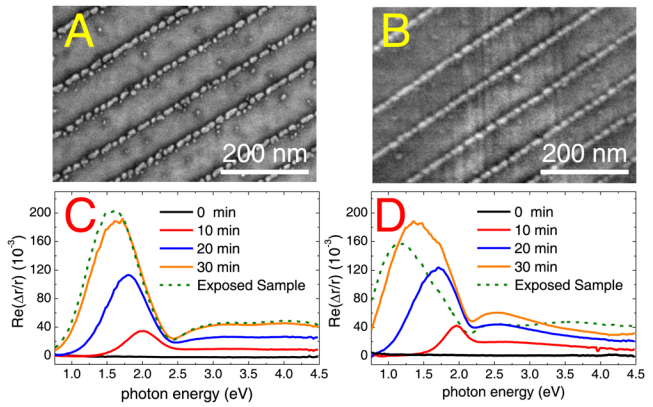

FIG. 3. (Color online) SEM images of Au (a) and Cu (b) NP arrays grown by glancing angle deposition with a 95 nm template periodicity. Au (c) and Cu (d) RAS spectra taken *in situ* at different deposition times and after exposure of the sample to ambient conditions.

geometry of the system expressed through the L_i^* coefficients, and the material properties via the other quantities. Fig. 2(a) shows the simulated absorption profile for identical spherical NP arrays supported on Al_2O_3 for light polarized along the array axis for different metals. The NP radius R was assumed to be 12 nm, the interparticle centre-to-centre distance was fixed to 25 nm, and the inter-array distance to 100 nm. It can be noted that different materials produce resonances at different energies as a consequence of their different dielectric properties. In Fig. 2(b), it is shown that the resonance position of the NP arrays when L^* is varied. Once the exciting light is polarized along the array axes, both increases of the aspect ratio along the same direction and stronger interactions between NPs result in lower L^*. Resonances over the whole visible range can in principle be realised.

Stepped Al_2O_3 (0001) substrates, miscut 6° along the $[1\bar{2}10]$ direction (MTI corp., USA), were obtained by annealing in atmosphere at 1420 °C for 24 h.[10] Samples were loaded into a high vacuum chamber (base pressure 2×10^{-8} mbar), and collimated adatoms were deposited at a tilted 6° angle with respect to the average surface orientation. Constant deposition rates on a substrate perpendicular to the collimated beam of $F = 0.23$ nm/min were measured, and a deposition time of 30 min was used. Figure 3 shows a scanning electron microscope (SEM) image of the resulting morphologies obtained by glancing angle deposition of Au and Cu. The steps are decorated by NP arrays elongated along the chain axis. Glancing angle deposition is thus virtually independent on the material deposited. The method was tested for different elements and NP arrays could be produced, provided the deposition parameters were optimised. Au and Cu were finally chosen as they survive atmospheric exposure and produce narrow resonances in the visible range, in accordance with Fig. 2(a). The average NP dimensions are below lithographic resolution (see Table I), and the surface morphology remains unchanged throughout the entire 5×5 mm^2 sample. The ratio between the diameter and average interparticle separation is 5.5 and 8 for Au and Cu, respectively; a strong field enhancement is thus expected.[7]

The optical features were measured *in situ* using RAS. RAS measures the difference of the in-plane complex reflection coefficients r_i measured along two orthogonal directions, normalised to the overall reflection at normal incidence. The positive direction is related to the direction along the array axis. After deposition, the recorded spectra show only positive peaks. The sharp resonances at low energies represent the plasmonic resonances along the array axes, while the additional positive features at higher energies are related to inter band contributions. For any enhancement spectroscopy, the exciting light needs to be polarized along the arrays axes and RAS can then measure its resonance position directly during the growth.

The plasmonic peaks measured by RAS appear broader than shown in Fig. 2(a) due to the increased scattering rate at the NP boundaries and to size distribution. The peak intensities increase with the amount of deposited material and the plasmonic peaks red shift for both Au and Cu, due to increases in the NP volume and, hence, in the coupling between neighbouring NPs.[10] The peaks are shifted further in the IR if compared with Fig. 2(a) as a result of the NP elongation along the array axis. The exposure of the sample to the atmosphere produced additional spectral changes, with the positive peaks red shifting by 0.04 eV for Au and by 0.26 eV for Cu. These modifications are attributed to the creation of an oxide/sulphide layer surrounding particles,[14,15]

TABLE I. The number of particles N per unit area, the average center to center distance l, and semiaxes R along (x) and perpendicular (y) to the array axes, for Cu and Au samples grown at glancing angle of incidence. An effective shape depolarization factor $1/L_x^*$ has been calculated using the same morphology. For the calculation, it was assumed $R_z = 5$ nm and ε_s being a homogeneous mixture of air and Al_2O_3 in order to take into account for the presence of the steps.

	N (NPs/μm^{-2})	l_y (nm)	l_x (nm)	R_x (nm)	R_y (nm)	$1/L_x^*$
Au	421 ± 140	95 ± 22	25 ± 6	11 ± 3	7 ± 2	15
Cu	390 ± 130	95 ± 22	27 ± 6	12 ± 3	8 ± 1	17

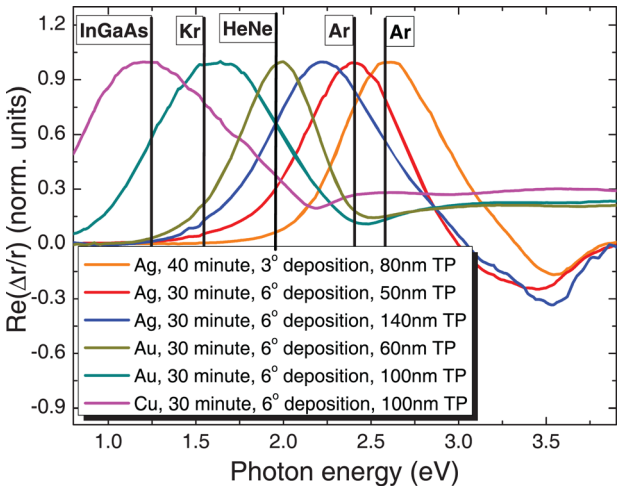

FIG. 4. (Color online) RAS spectra of samples after exposure of the samples to the atmosphere. The NP arrays were produced using different metals, template periodicities, and deposition angles and times. Vertical lines represent energies of common lasers.

confirming Cu is particularly reactive to atmospheric exposure.

The fine tuning of the spectral resonance position in the visible range is obtained by modifying L^* as suggested in Fig. 2(b). This has been realised by changing in the deposition parameters, resulting in different NP morphologies and interparticle distances. The resulting optical response is shown in Fig. 4, where the normalized RAS spectra for various deposition parameters of NP arrays made of Ag, Au, and Cu are presented. Ag NP arrays result in positive resonances placed at higher energy, in accordance with Fig. 2(a). Negative peaks related to resonances perpendicular to the array axes can also be observed due to the absence of interband related structures. Larger template periodicities (TPs) result in red shifts of the resonances along the array axes. The right combination of material and deposition parameters allows one to produce structures with a resonance energy matching the particular laser line used. At the same time, RAS can be used to measure the resonance profile during growth and also estimate the NP morphological dispersion via the Gaussian broadening of the peaks.[10] The current experimental arrangement does not allow the substrate temperature to be varied during deposition. However, we believe that deposition on substrates at higher temperatures could further increase the order of the NP arrays and result in narrower resonance profiles.

In conclusion, we described a self-organized approach for the large scale physical synthesis of anisotropic plasmonic NP arrays supported on a dielectric substrate. The technique is independent of the deposited material and could also be generalized to different substrates, obtained by patterning of the surface using low-angle ion sputtering.[12] The resulting structures present strong dichroic plasmonic resonances, and they offer themselves naturally as candidates for enhanced spectroscopy. The exact resonance energy required can be obtained by choosing the appropriate material and deposition parameters. RAS can measure the resonance profile during the growth, and the deposition can be interrupted to obtain structures with the required resonances. The produced NP arrays can also be used as a building block for waveguiding applications or as catalysts for the growth of low-dimensional out-of-plane structures, such as ZnO.[18] Finally, by combining different materials, core/shell metamaterials could be grown utilising this method.

Thanks to J. F. McGilp for the useful discussions. This work is supported by SFI 06/IN.1/I01 and the INSPIRE programme under the Irish Government's PRTLI Cycle 4 (NDP 2007-2013). O. Ualibek acknowledges the support of the Government of Republic of Kazakhstan under Bolashak programme.

[1]S. Maier, P. Kik, H. A. Atwater, and S. Meltzer, Nature Mater. **2**, 229 (2003).
[2]H. A. Atwater and A. Polman, Nature Mater. **9**, 205 (2010).
[3]A. Wei, B. Kim, B. Sadtler, and S. L. Tripp, ChemPhysChem **2**, 743 (2001).
[4]P. Pompa, L. Martiradonna, A. D. Torre, F. Sala, L. Della Manna, M. De Vittorio, F. Calabi, R. Cingolani, and R. Rinaldi, Nat. Nanotechnol. **1**, 126 (2006).
[5]N. Félidj, J. Aubard, G. Lévi, J. R. Krenn, A. Hohenau, G. Schider, A. Leitner, and F. R. Aussenegg, Appl. Phys. Lett. **82**, 3095 (2003).
[6]F. J. García-Vidal and J. B. Pendry, Phys. Rev. Lett. **77**, 1163 (1996).
[7]D. A. Genov, A. K. Sarychev, V. M. Shalaev, and A. Wei, Nano Lett. **4**, 153 (2004).
[8]Z. Nie, A. Petukhova, and E. Kumacheva, Nat. Nanotechnol. **5**, 15 (2009).
[9]F. Cuccureddu, S. Murphy, I. Shvets, M. Porcu, and H. W. Zandbergen, Nano Lett. **8**, 3248 (2008).
[10]R. Verre, K. Fleischer, R. G. S. Sofin, N. McAlinden, J. F. McGilp, and I. V. Shvets, Phys. Rev. B **83**, 125432 (2011).
[11]R. Verre, K. Fleischer, C. Smith, N. McAlinden, J. F. McGilp, and I. V. Shvets, Phys. Rev. B **84**, 085440 (2011).
[12]S. Camelio, D. Babonneau, D. Lantiat, L. Simonot, and F. Pailloux, Phys. Rev. B **80**, 155434 (2009).
[13]T. Oates, A. Keller, S. Facsko, and A. Mcklich, Plasmonics **2**, 47 (2007).
[14]R. Verre, K. Fleischer, J. F. McGilp, D. Fox, H. Behan, G. Zhang, and I. V. Shvets, Nanotechnology **23**, 035606 (2012).
[15]C. Bohren and D. Huffman, *Absorption and Scattering of Light by Small Particles* (Wiley, New York, 1983).
[16]P. B. Johnson and R. W. Christy, Phys. Rev. B **6**, 4370 (1972).
[17]E. Palik, *Handbook of Optical Constants of Solids III* (Elsevier, New York, 1998).
[18]Y. Zhang, H. Jia, R. Wang, C. Chen, X. Luo, D. Yu, and C. Lee, Appl. Phys. Lett. **83**, 4631 (2003).